Cancer Cell, Volume *41*

Supplemental information

Anti-PD-1 immunotherapy with androgen deprivation therapy induces robust immune infiltration in metastatic castration-sensitive prostate cancer

Jessica E. Hawley, Aleksandar Z. Obradovic, Matthew C. Dallos, Emerson A. Lim, Karie Runcie, Casey R. Ager, James McKiernan, Christopher B. Anderson, Guarionex J. Decastro, Joshua Weintraub, Renu Virk, Israel Lowy, Jianhua Hu, Matthew G. Chaimowitz, Xinzheng V. Guo, Ya Zhang, Michael C. Haffner, Jeremy Worley, Mark N. Stein, Andrea Califano, and Charles G. Drake

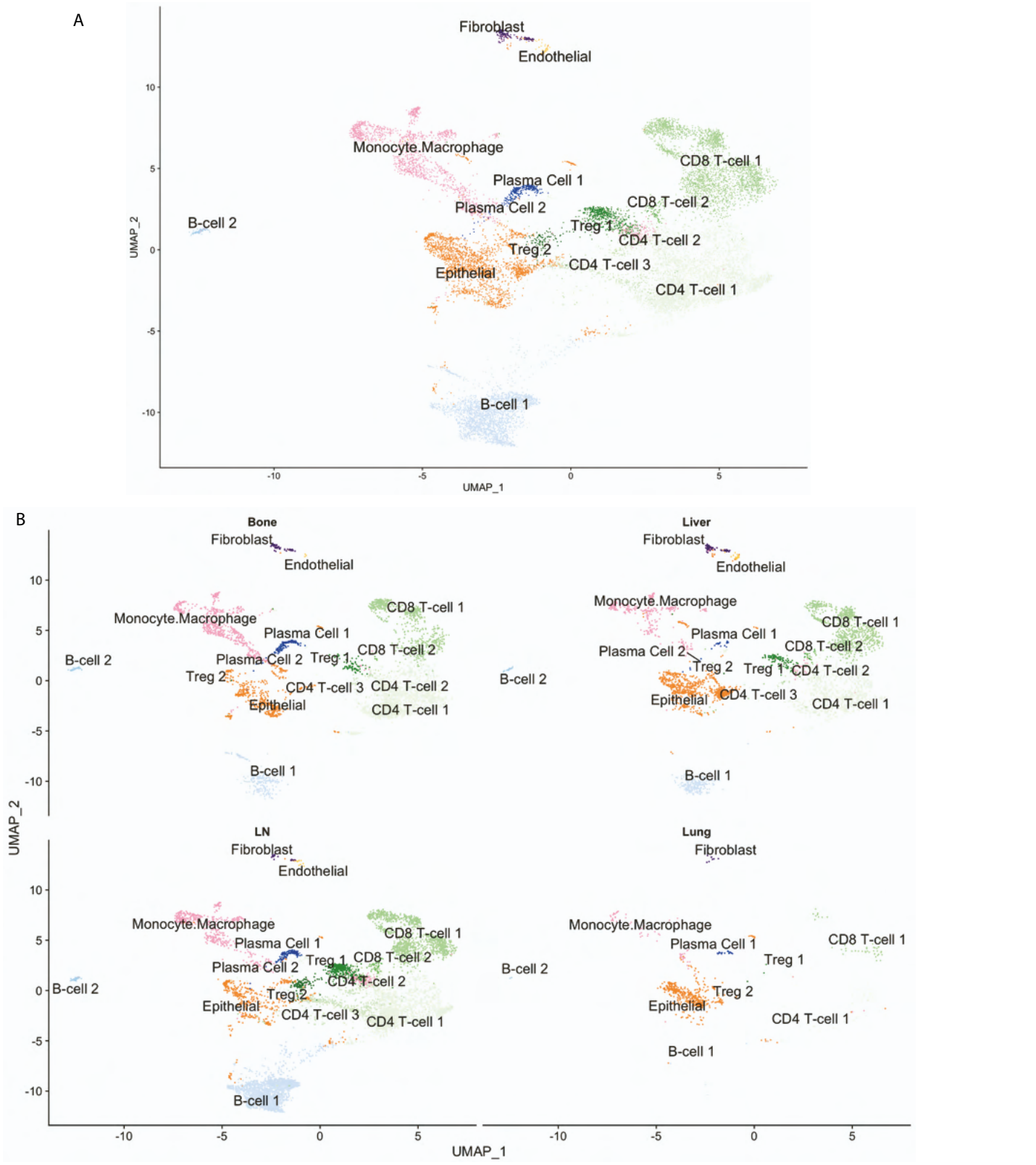

Figure S1: Gene Expression Clustering, Related to Figure 1.
A) UMAP plot showing clustering of all cells in tumor microenvironment across all patients, clustered on gene expression instead of VIPER-inferred protein activity. Cell types are inferred by SingleR. Total number of clusters is smaller than clustering in Figure 1 on VIPER-inferred protein activity. B) UMAP plot from A, split by metastatic tissue site.

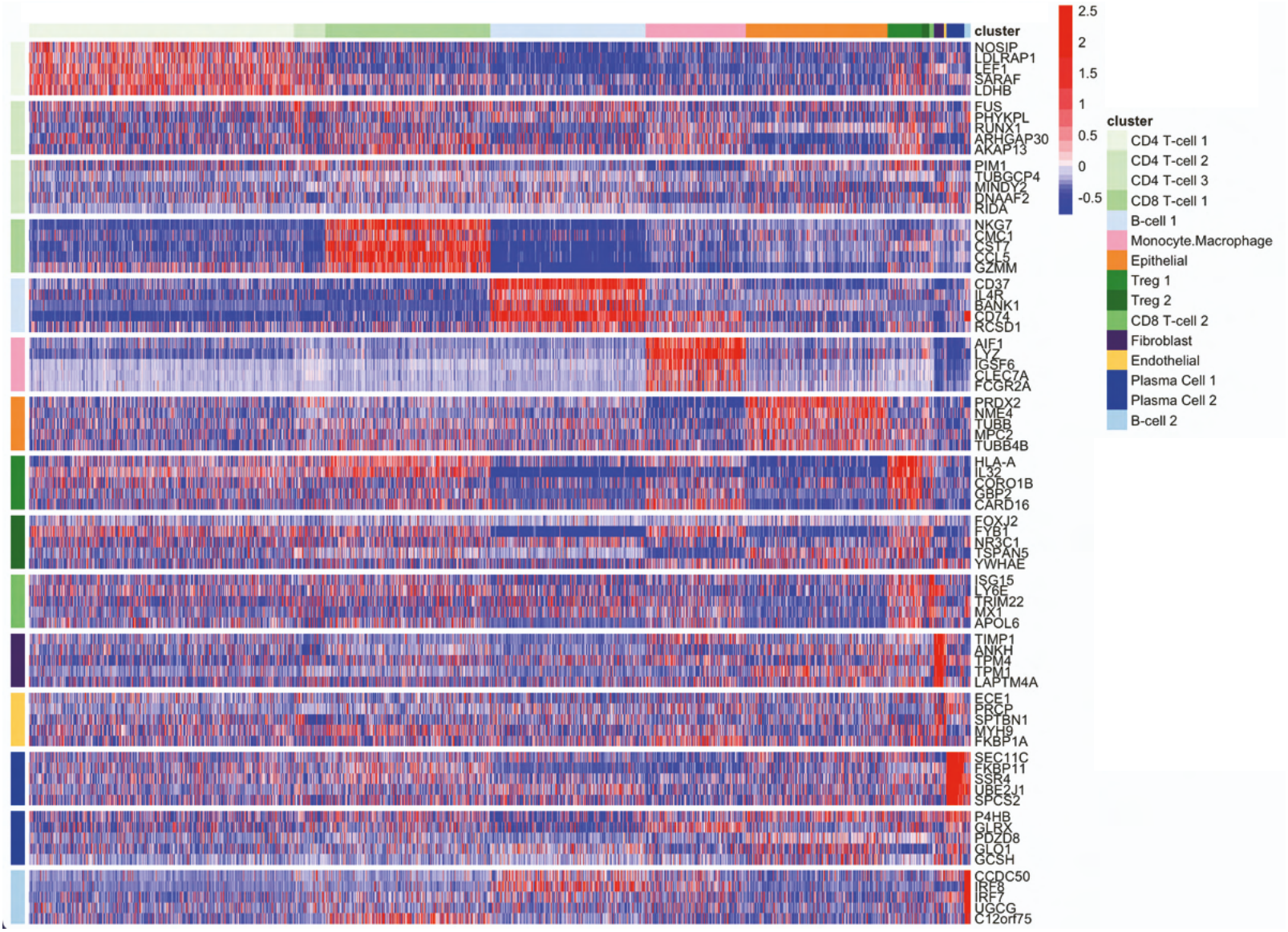

Figure S2: Top Gene Expression Cluster Markers, Related to Figure 2
Heatmap of top 5 most differentially upregulated genes for each cell type cluster from aggregate single-cell RNA-Sequencing data across all patient samples, with clusters corresponding to Figure S1. Each row represents a protein, grouped by cluster in which they are the most active, with cluster labels on the x and y-axes.

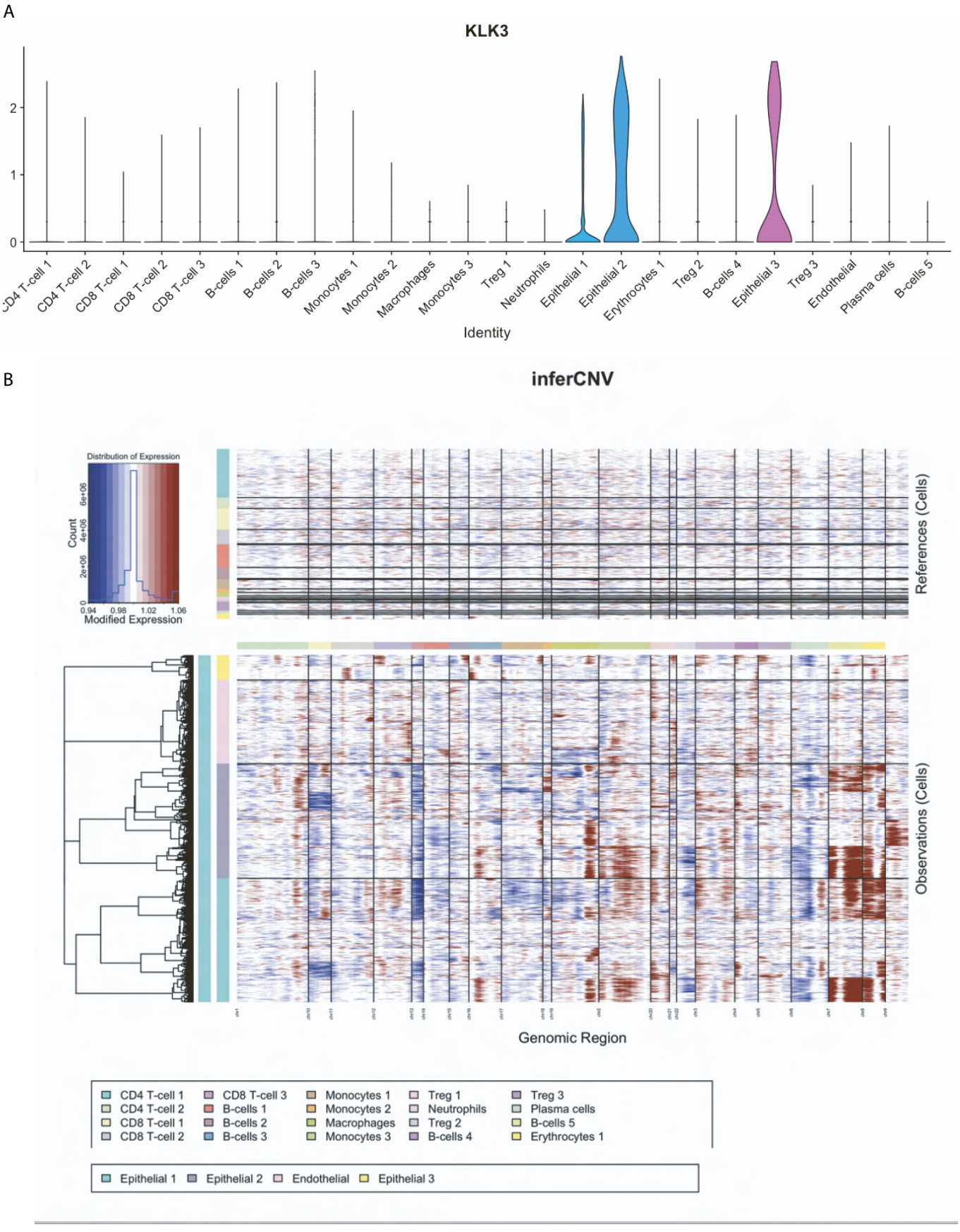

Figure S3: Identification of Tumor Cells by Marker Expression and Copy Number Variation, Related to Figure 6
A) log10 normalized expression of prostate cancer tumor marker protein KLK3 in each cell cluster identified by VIPER, such that expression is non-zero only in Epithelial cell clusters. B) InferCNV plot of cell-by-cell copy number variations, where all immune-lineage cells are taken as a copy-number-normal reference for inference of variations in copy number in Epithelial cell clusters and Endothelial cell cluster as a control. Each epithelial cell cluster is notable copy number aberrant across multiple chromosomes, while endothelial cells are grossly copy number normal.

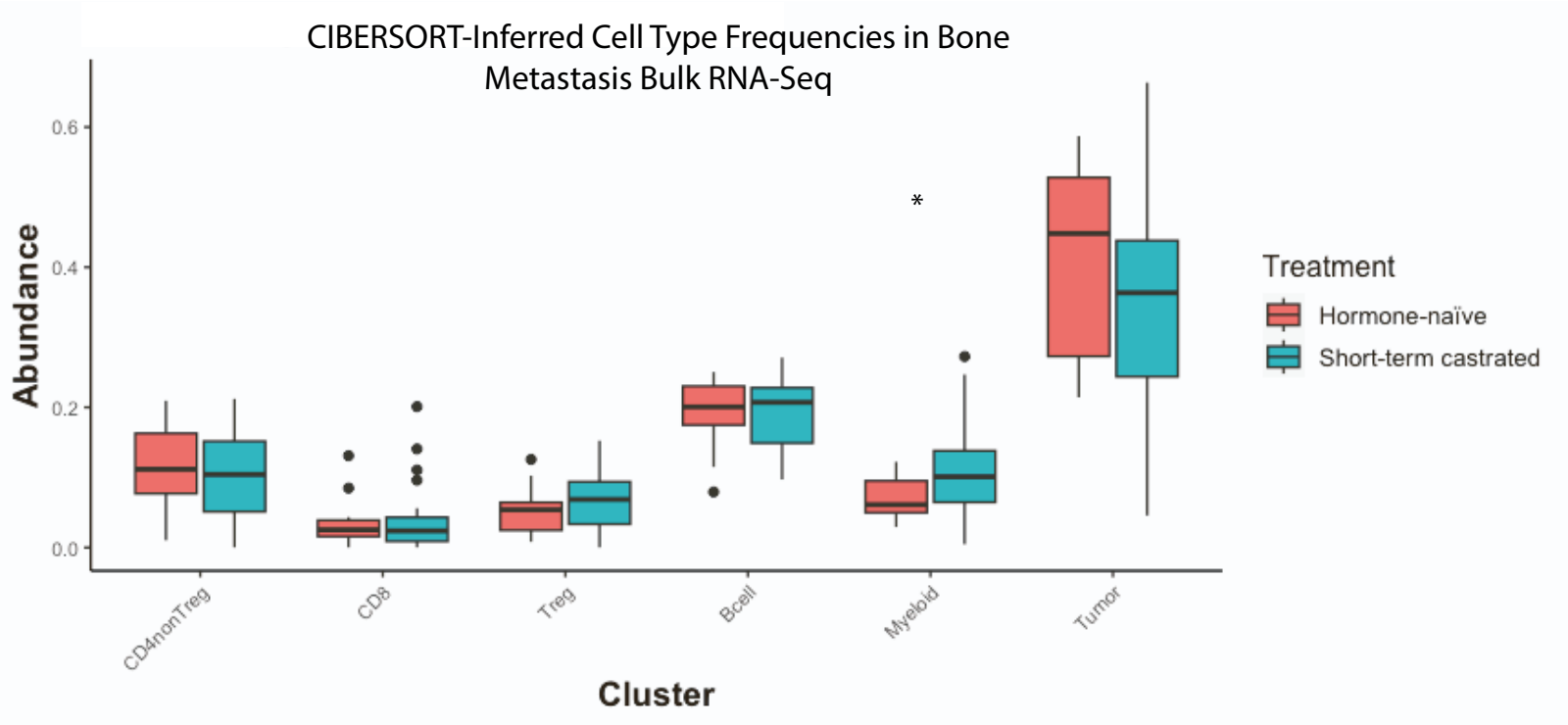

Figure S4: Inferred Cell Type Frequencies in bulkRNA-Seq Bone Metastasis Data, Related to Figure 3
Cell Type frequencies inferred by CIBERSORTx from a cohort of n=17 hormone naïve castrate-sensitive bone metastases and n=21 short-term castrated samples 94 . As in Figure 3A-B, significant increase in myeloid infiltrate is observed with ADT ($p = 0.028$), with trend toward decrease in CD4 non-Tregs ($p = 0.37$) and Tumor cells ($p = 0.14$). Statistically significant results ($p<0.05$ by Wilcox test) comparing inferred frequency in hormon

Hallmarks of Cancer Pathway Enrichment

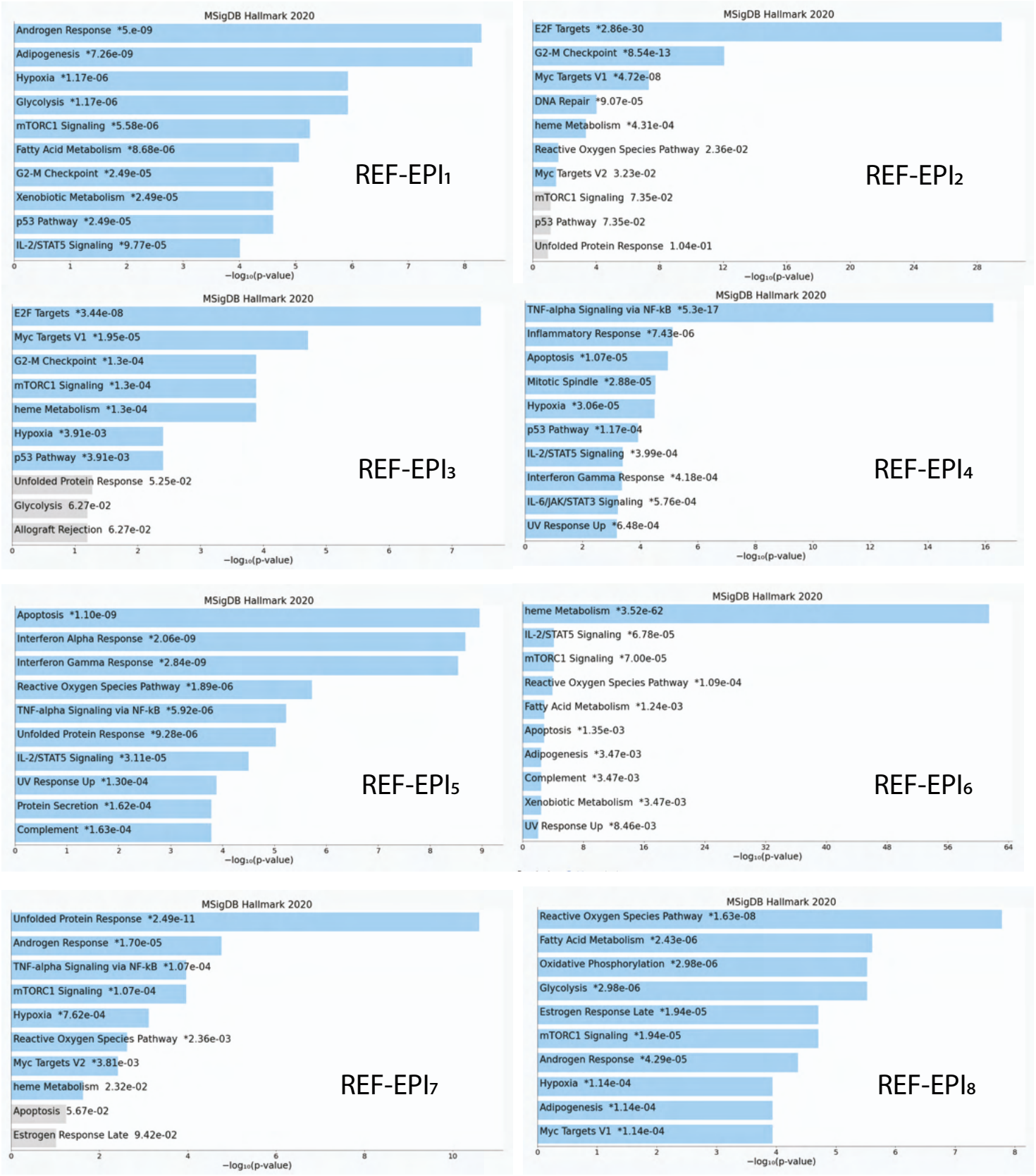

Figure S5: Hallmarks of Cancer Enriched Pathways in Tumor Cell Subclusters, Related to Figure 6
For each tumor cell subcluster identified in Figure 6, plots of the top 10 enriched pathways from Hallmarks of Cancer. Pathway enrichment is computed on genes differentially expressed in each tumor subcluster relative to other tumor subclusters. -Log10(p-values) are plotted on the x-axes, such that statistically significant enriched pathways are shaded in blue.

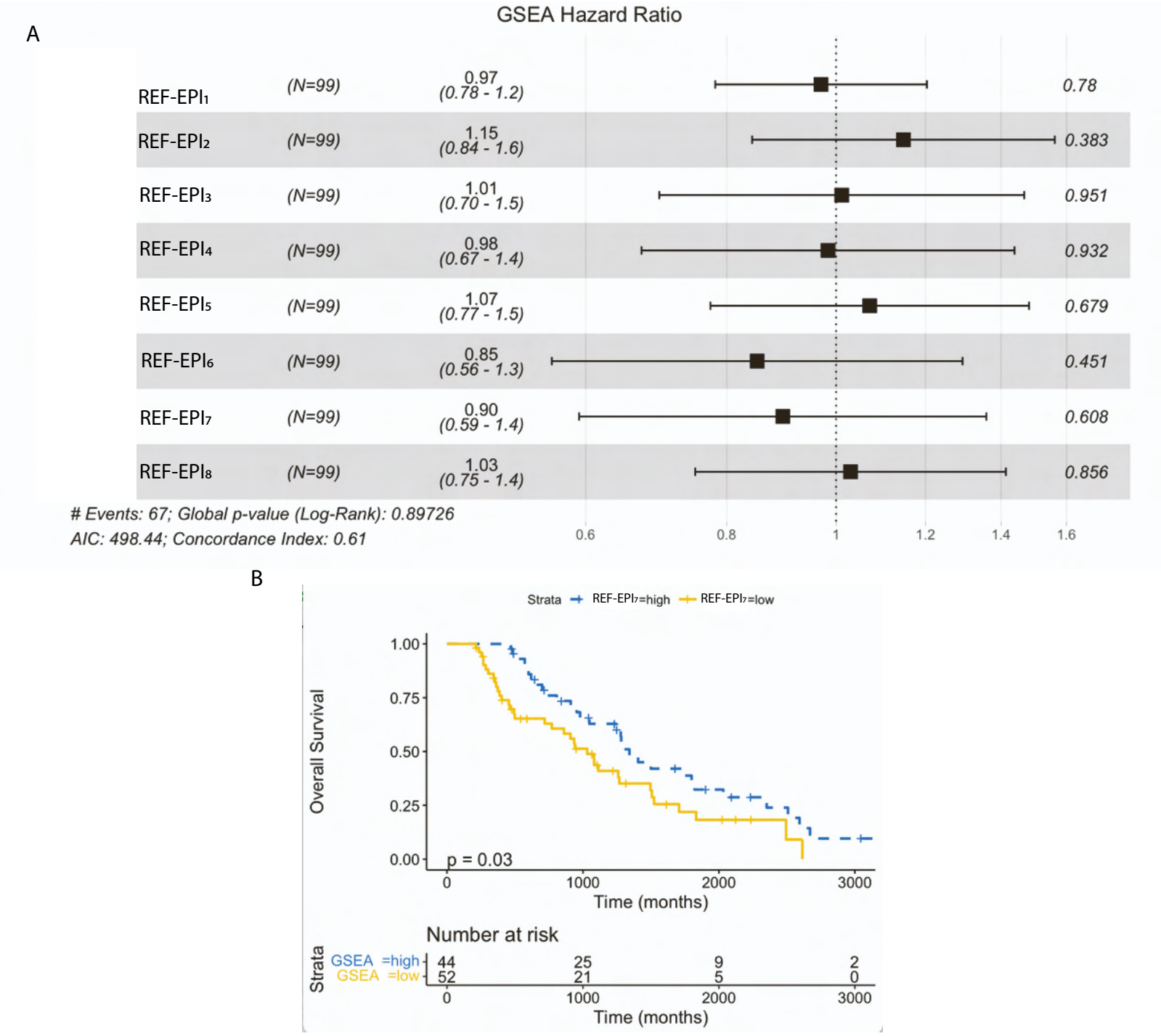

Figure S6: Tumor Single-Cell Subcluster Signatures and Outcome in West Coast SU2C, Related to Figure 7
A) Forest plot of Cox regression hazard ratios testing association in West Coast Stand Up to Cancer (SU2C) dataset of patient-by-patient Normalized Enrichment Score for each tumor subcluster gene set with overall survival. B) Kaplan-Meier curve testing association of binarized REF-EPI 7 gene set enrichment (greater than 0 = high, less than 0 = low) with survival, such that REF-EPI 7 enrichment significantly associates with improved survival. Kaplan-Meier curves are not shown for the remaining clusters as log-rank p-values for these were not statistically significant ($p>0.05$).

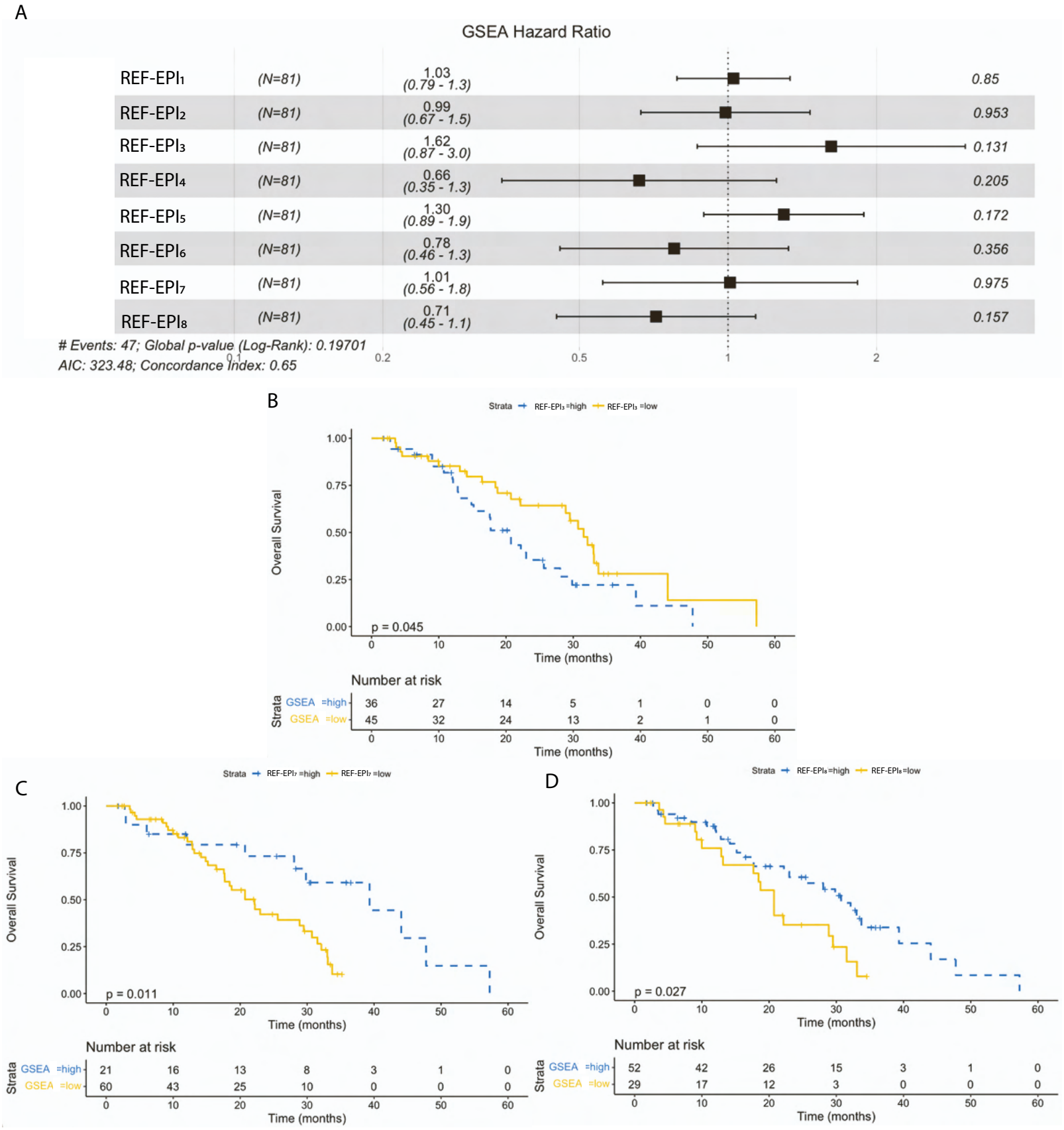

Figure S7: Tumor Single-Cell Subcluster Signatures and Outcome in East Coast SU2C, Related to Figure 7

A) Forest plot of Cox regression hazard ratios testing association in East Coast Stand Up to Cancer (SU2C) dataset of patient-by-patient Normalized Enrichment Score for each tumor subcluster gene set with overall survival.

B) Kaplan-Meier curve testing association of binarized REF-EPI 3 gene set enrichment (greater than 0 = high, less than 0 = low) with survival, such that REF-EPI 3 enrichment significantly associates with worse survival. C) Kaplan-Meier curve testing association of binarized REF- EPI 7 gene set enrichment (greater than 0 = high, less than 0 = low) with survival, such that REF-EPI 7 enrichment significantly associates with improved survival. D) Kaplan-Meier curve testing association of binarized REF-EPI 8 gene set enrichment (greater than 0 = high, less than 0 = low) with survival, such that REF-EPI 8 enrichment significantly associates with improved survival. Kaplan-Meier curves are not shown for the remaining clusters as log-rank p-values for these were not statistically significant (p>0.05).